107° CONGRESSO NAZIONALE SIF

13-17 settembre 2021

Point defects in silicon for quantum technologies at room temperature

Simona Achilli[1], Nguyen H. Le[2], Guido Fratesi[1], Nicola Manini[1], Giovanni Onida[1], Marco Turchetti[3,4,5], Giorgio Ferrari[4], Takahiro Shinada[6], Takashi Tanii[7], Enrico Prati[3]

[1]*Dipartimento di Fisica, **Università degli Studi di Milano**, Italy.*
[2]*Advanced Technology Institute and Department of Physics, **University of Surrey**, United Kingdom.*
[3]*Istituto di Fotonica e Nanotecnologie, **Consiglio Nazionale delle Ricerche**, Italy.*
[4]*Dipartimento di Elettronica, Informazione e Bioingegneria, **Politecnico di Milano**, Italy.*
[5]*CountryResearch Laboratory of Electronics, **Massachusetts Institute of Technology**, USA.*
[6]*Center for Innovative Integrated Electronic Systems (CIES), **Tohoku University**, Japan.*
[7]*Faculty of Science and Engineering, **Waseda University**, Japan.*
Email: simona.achilli@unimi.it

ETSF

UNIVERSITÀ DEGLI STUDI DI MILANO
Dipartimento di Fisica

The quantum technologies roadmap

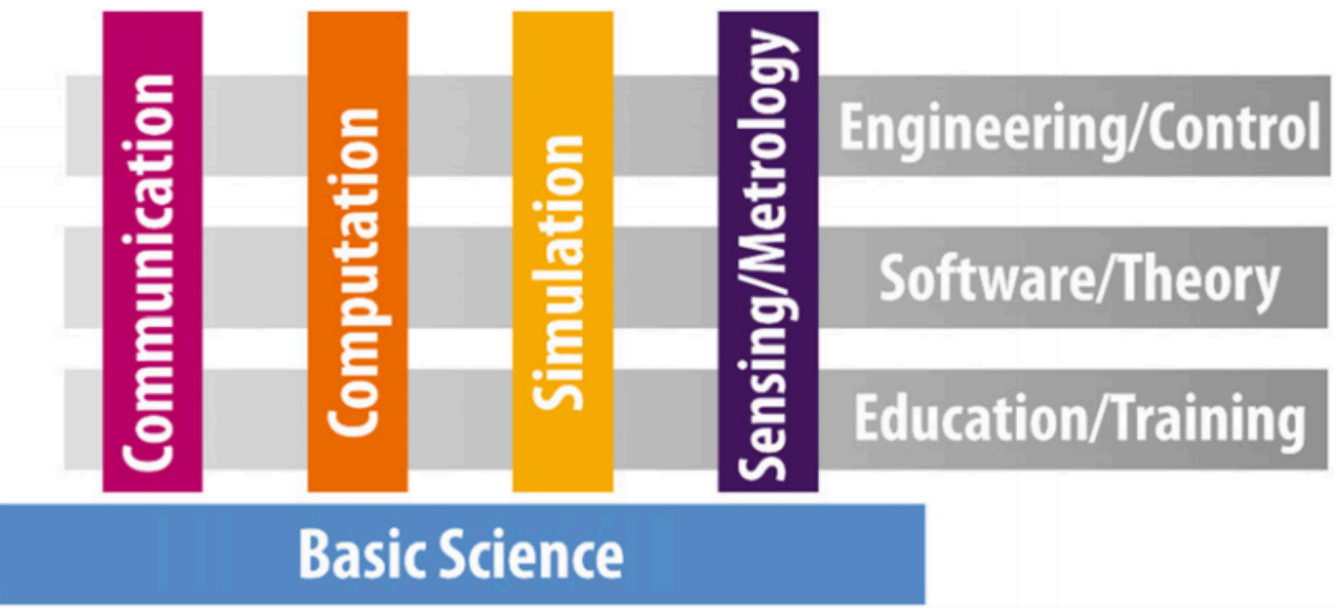

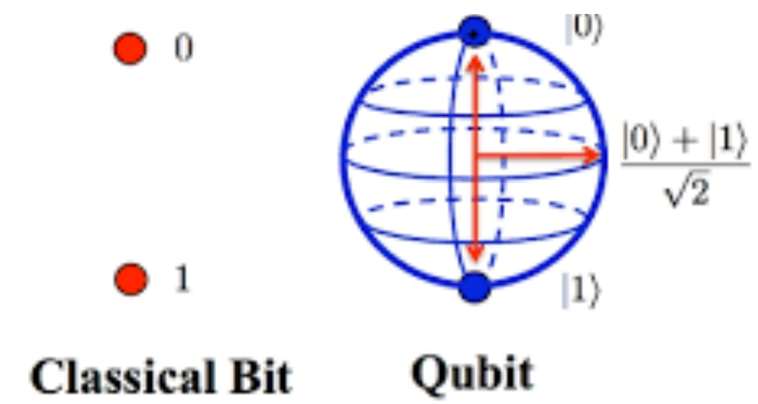

Physical qubit roadmap for quantum computer

Di Vincenzo criteria for qubits

- Scalable system
- Initialization/readout
- Long decoherence time
- Universal set of quantum gate
- Qubit specific measurements

…and "industrial" needs

- Integrable in existing production technologies
- Operating at ambient conditions

(Source: Quantum Technologies 2020 report, Yole Développement)

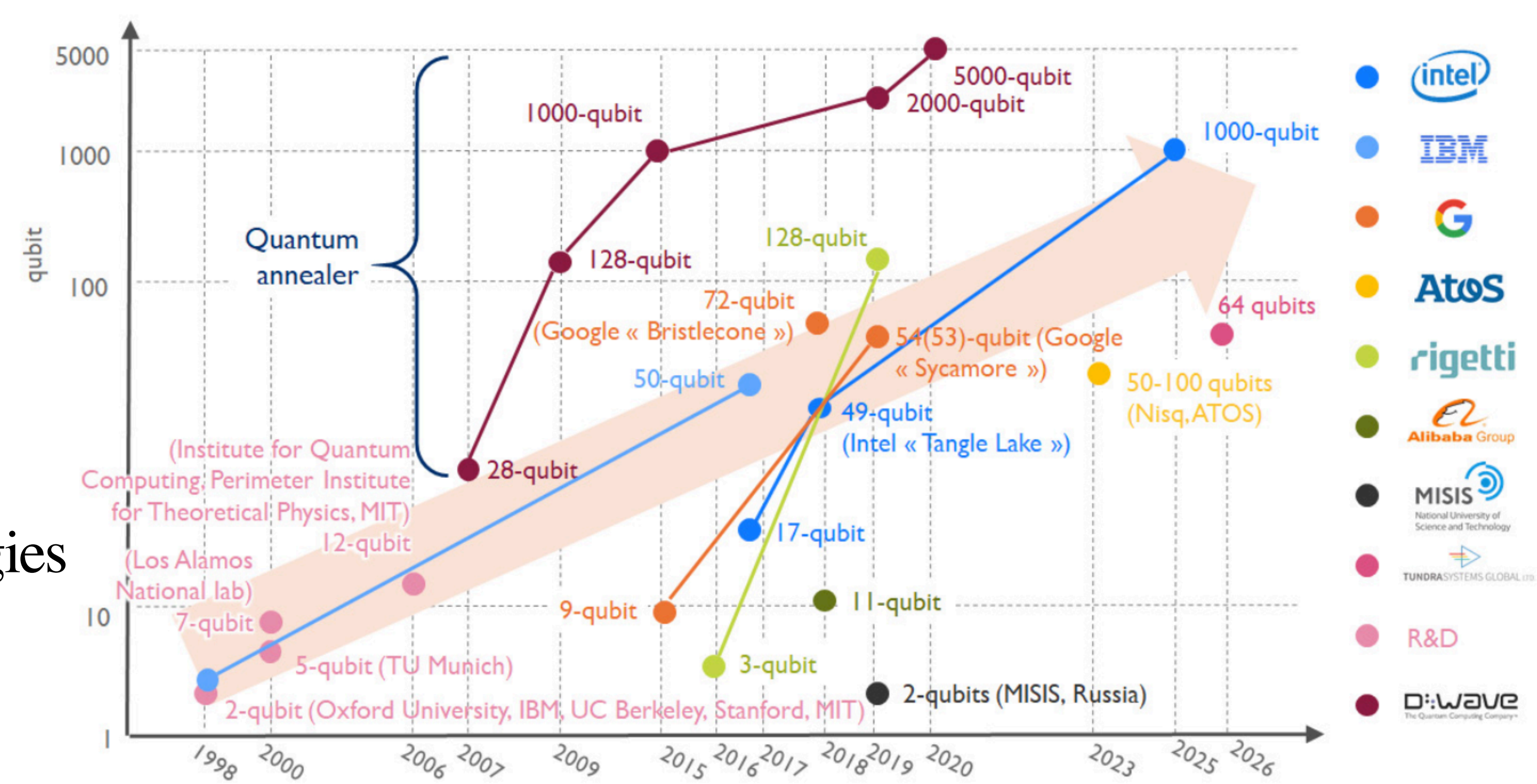

Point defects in semiconductors for encoding quantum information

- Two level systems based on electronic/nuclear spin
- Single photon emitters
- Initialization and read out: —> Optical spin manipulation
  —> Magnetic fields

NV center diamond

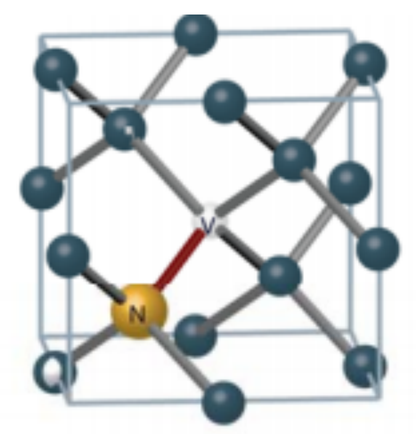

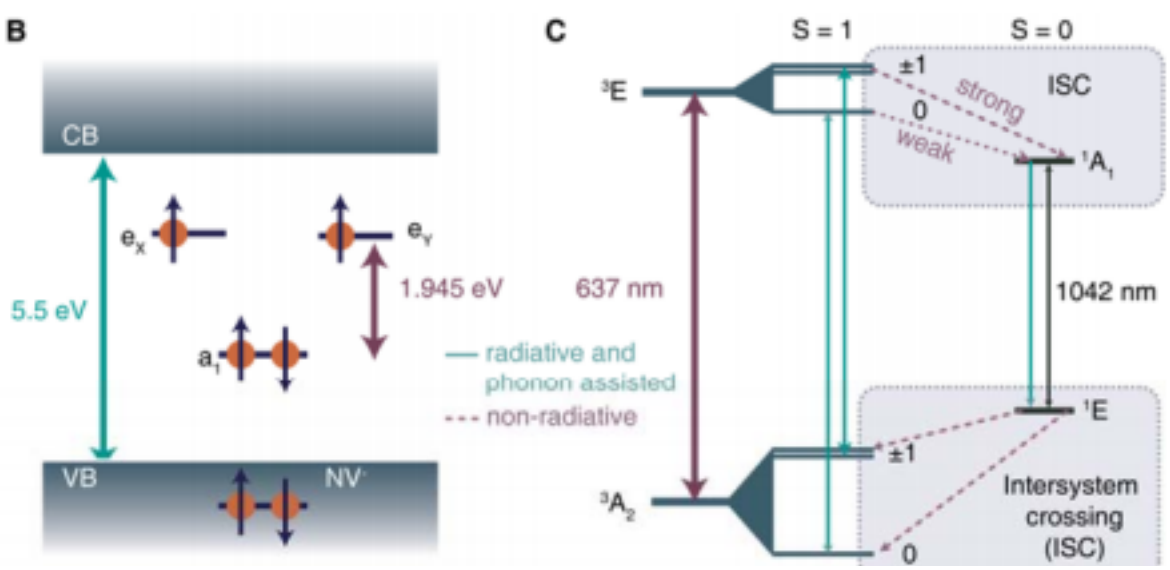

Donors silicon

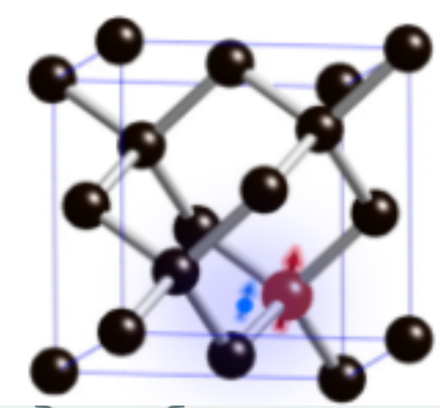

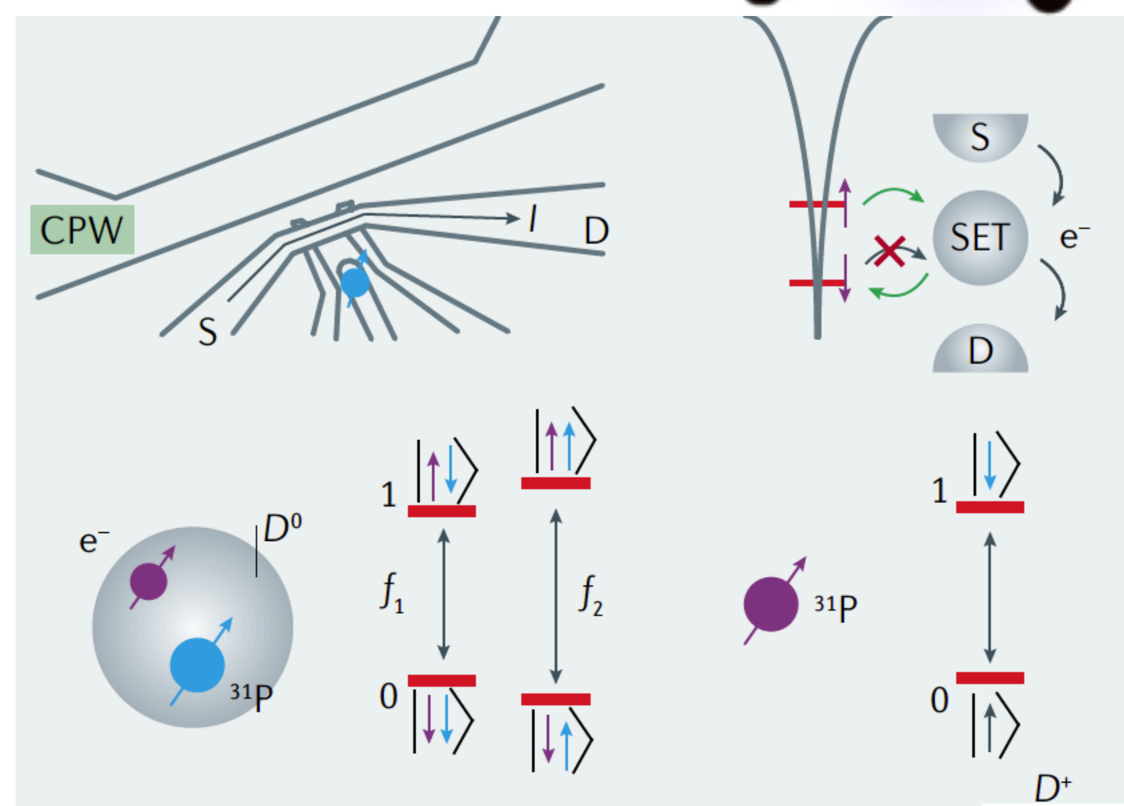

✗Not easily integrable in silicon industry

✗Operate at cryogenic temperature

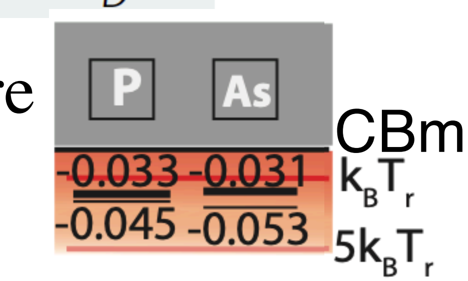

Point defects in semiconductors for encoding quantum information

- Two level systems based on electronic/nuclear spin
- Single photon emitters
- Initialization and read out: —> Optical spin manipulation
  —> Magnetic fields

NV center diamond

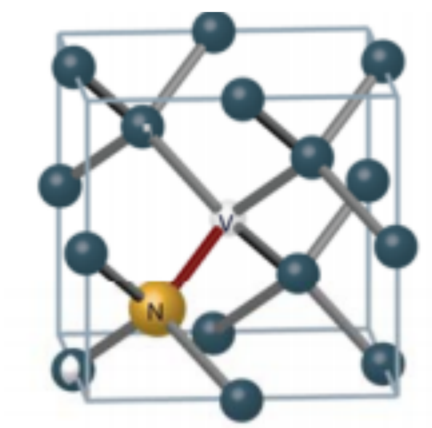

Donors silicon

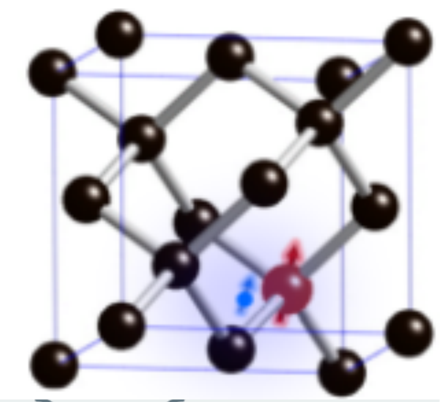

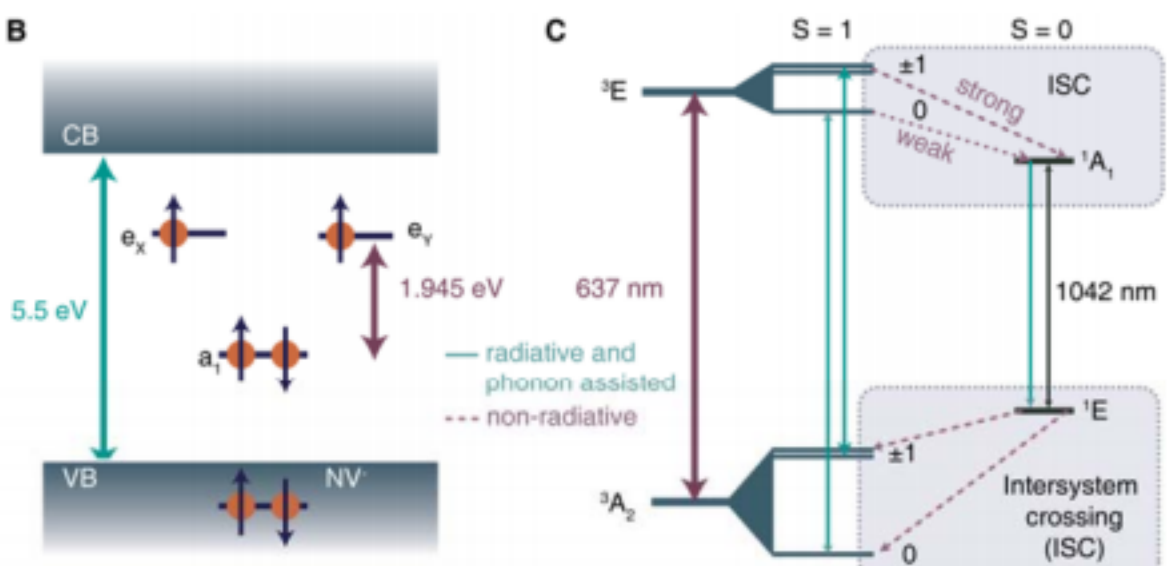

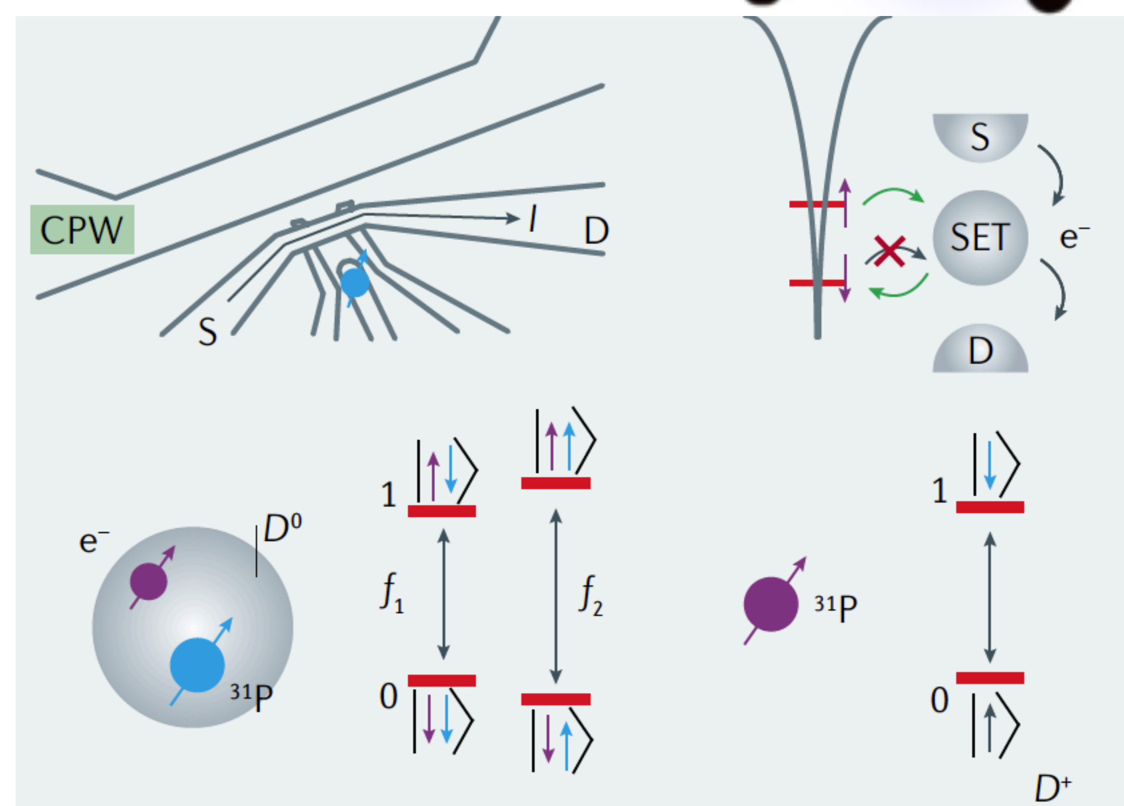

Deep impurities in silicon

✓ Room temperature operations
✓ Integrated in silicon industry

Ge-vacancy complexes

Obtained via Single Ion implantation technology —> accurate spatial control

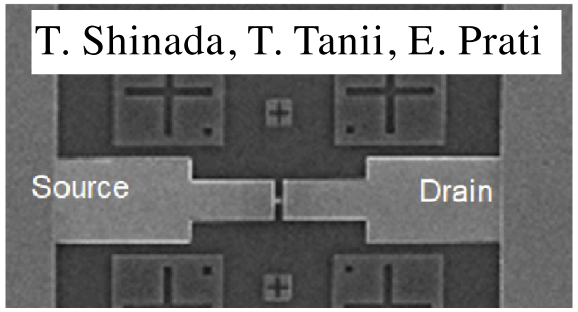

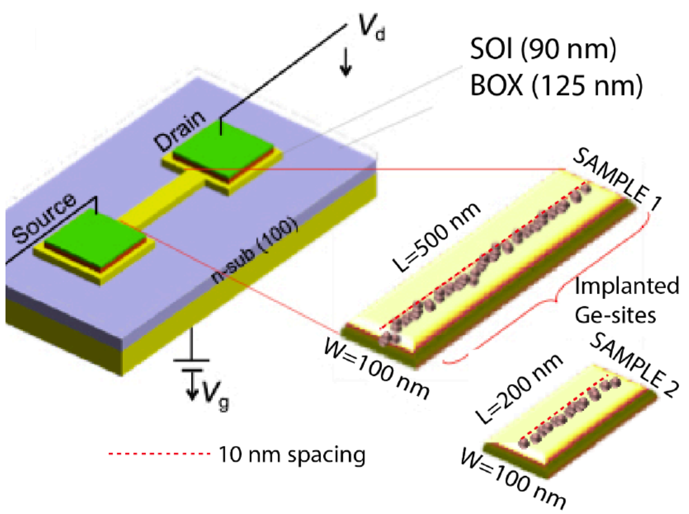

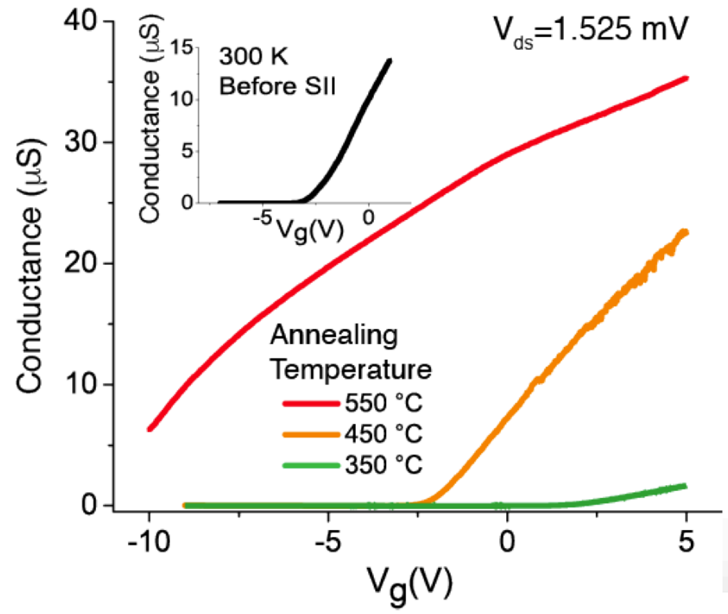

Low filling: E_a ~20 meV
(1.3 meV in Si:P)

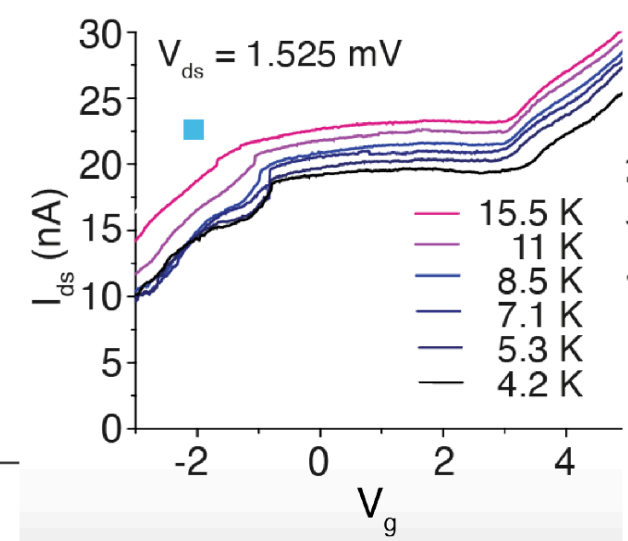

High filling: E_a ~ 1 meV
(6.8 meV in Si:P)

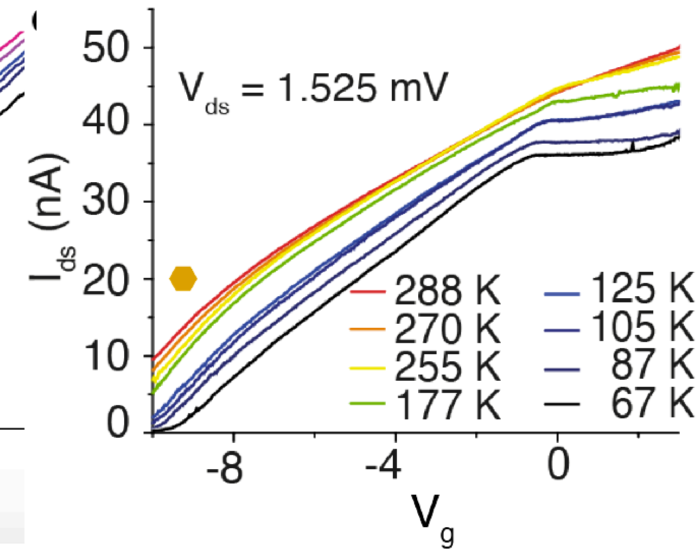

nffa.eu
nanoscience foundries & fine analysis

Objectives of the theoretical study

- Determine the defect stechiometry
- Characterize the electronic spectrum
- Explain the temperature activated conductivity

Theoretical "issues"

- Accurate description of the host properties —> silicon gap
- Charged excited states
- Manage defect-defect interaction —> dilute impurities
- Transport along a chain of defects

Aspects affecting I-V curves

- impurity states within the gap
- effect local environment
- inter-dot and intra-dot e-e interaction
- correlation
- disorder
- external bias
- coupling to the electrodes

The gap problem

$$E_g = -\,[(E_0(N) - E_0(N-1)) - (E_0(N+1) - E_0(N))] = AE - IE$$

Underestimated by DFT

	Energy	LDA	HF	Exp.	Hyb	LDA-1/2
Si	$E_{g,i}^{gKS}$	0.51	6.57	1.17	1.13	1.12

Phys. Rev. B **76**, 115109 (2007)

Hybrid Functionals

$$V_{Hybrid}: \quad \alpha E^x_{HF} + (\alpha - 1) E^x_{DFT} + E^c_{DFT}$$

Screened exchange: $\alpha = -1/\epsilon_\infty$

Computational costly —> small systems

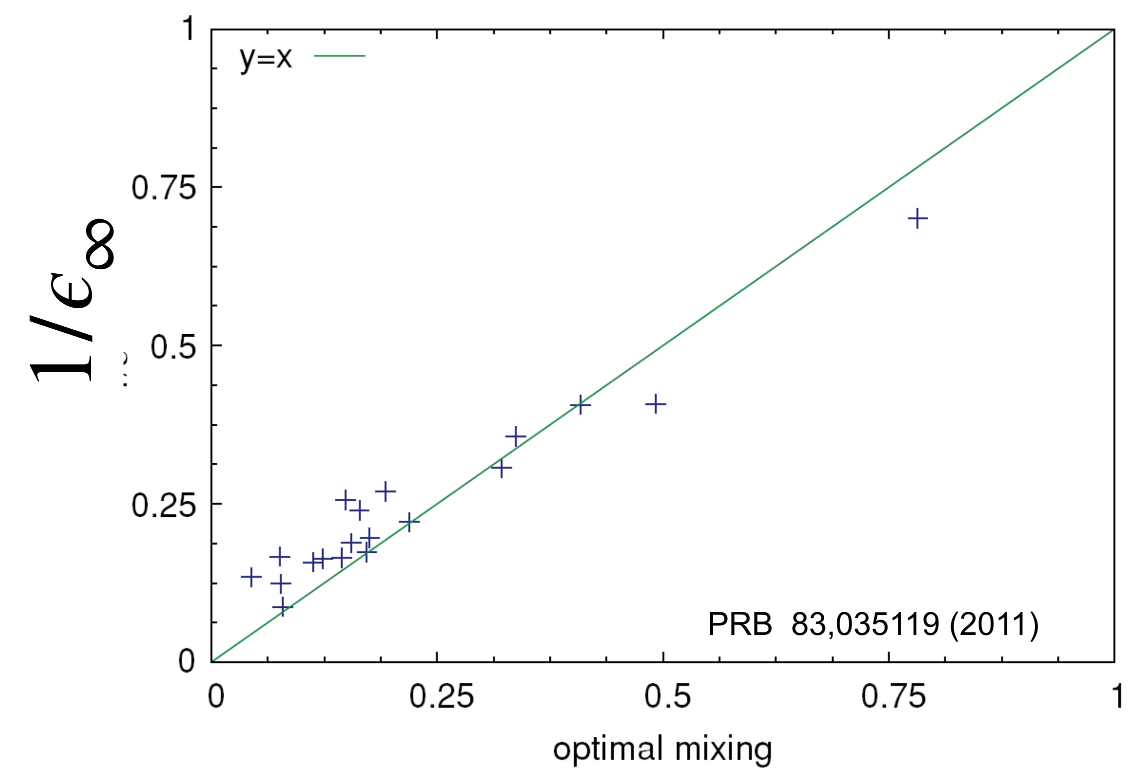

LDA-1/2

$$\frac{\delta E}{\delta f_a} = e_a(f_a)$$

$$E_\alpha(0) - E_\alpha(-1) = \epsilon_\alpha(0) + S_\alpha$$

$$S_\alpha = \int d^3r\, n_\alpha(\vec{r})[V(0,\vec{r}) - V(-1/2,\vec{r})]$$

(x $\Theta(r) = \begin{cases} \left[1 - \left(\frac{r}{CUT}\right)^m\right]^3 & r \le CUT \\ 0 & r > CUT \end{cases}$ in extended systems)

Self energy correction included in the pseudo - potential

No additional computational cost —> large cells

L. G. Ferreira et al., Phys. Rev. B 78, 125116 (2008)

Electronic properties - Charged excitations

Charge transition levels $\varepsilon(q|q') = \frac{E_F(q) - E_F(q')}{(q-q')} - E_{VBM}$

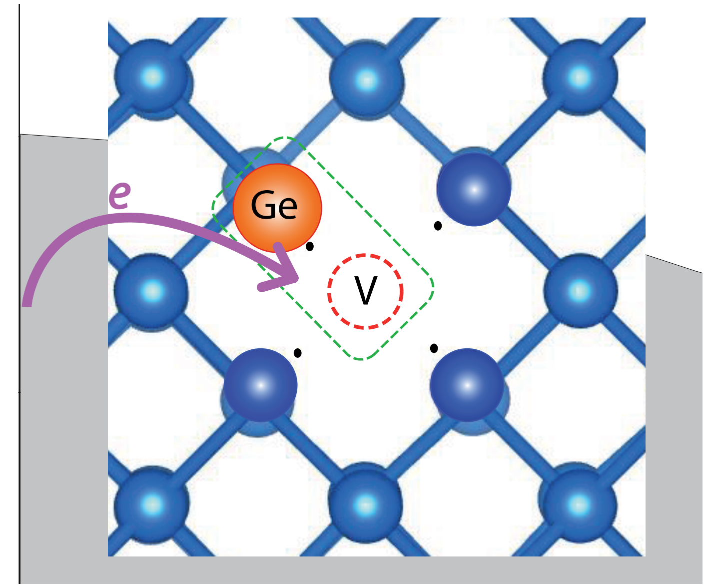

Janak theorem $E_F(q) - E_F(q') = \int_0^1 e_{LUMO}(N+n)dn$

$$E_F(q) - E_F(q') = \frac{e_{LUMO}(N) + e_{HOMO}(N+1)}{2}$$

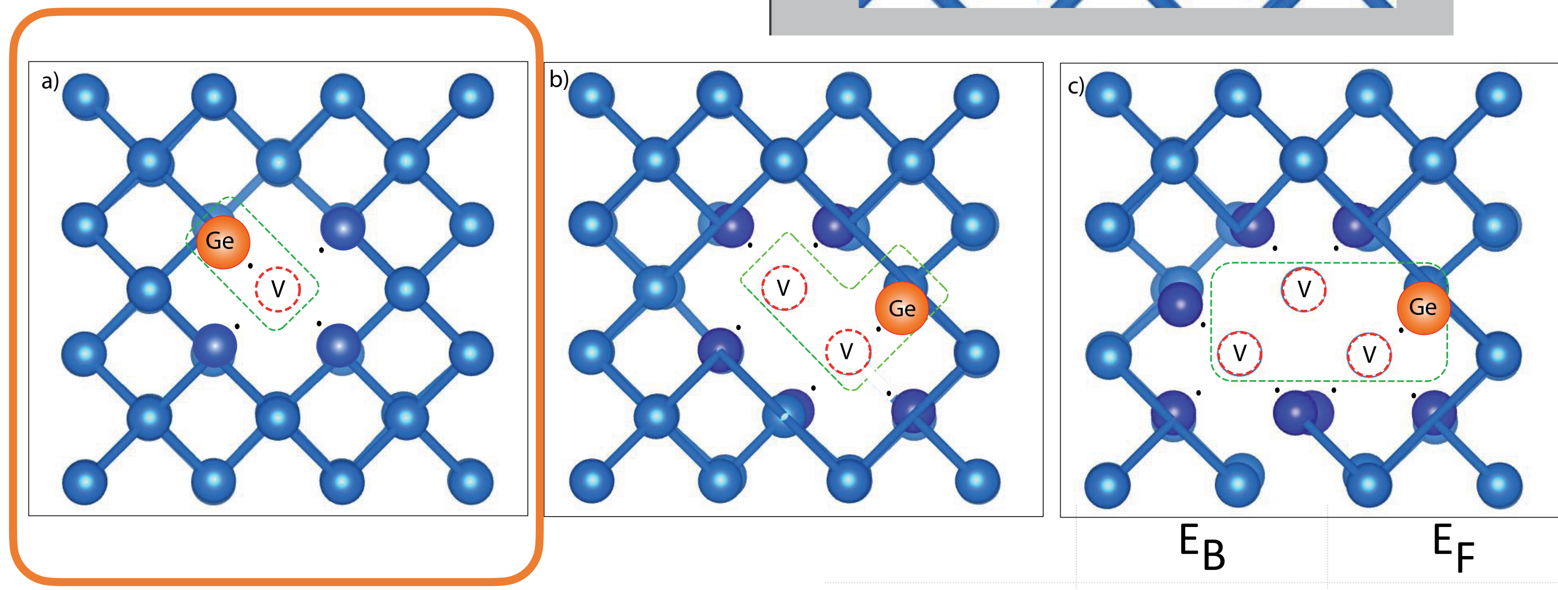

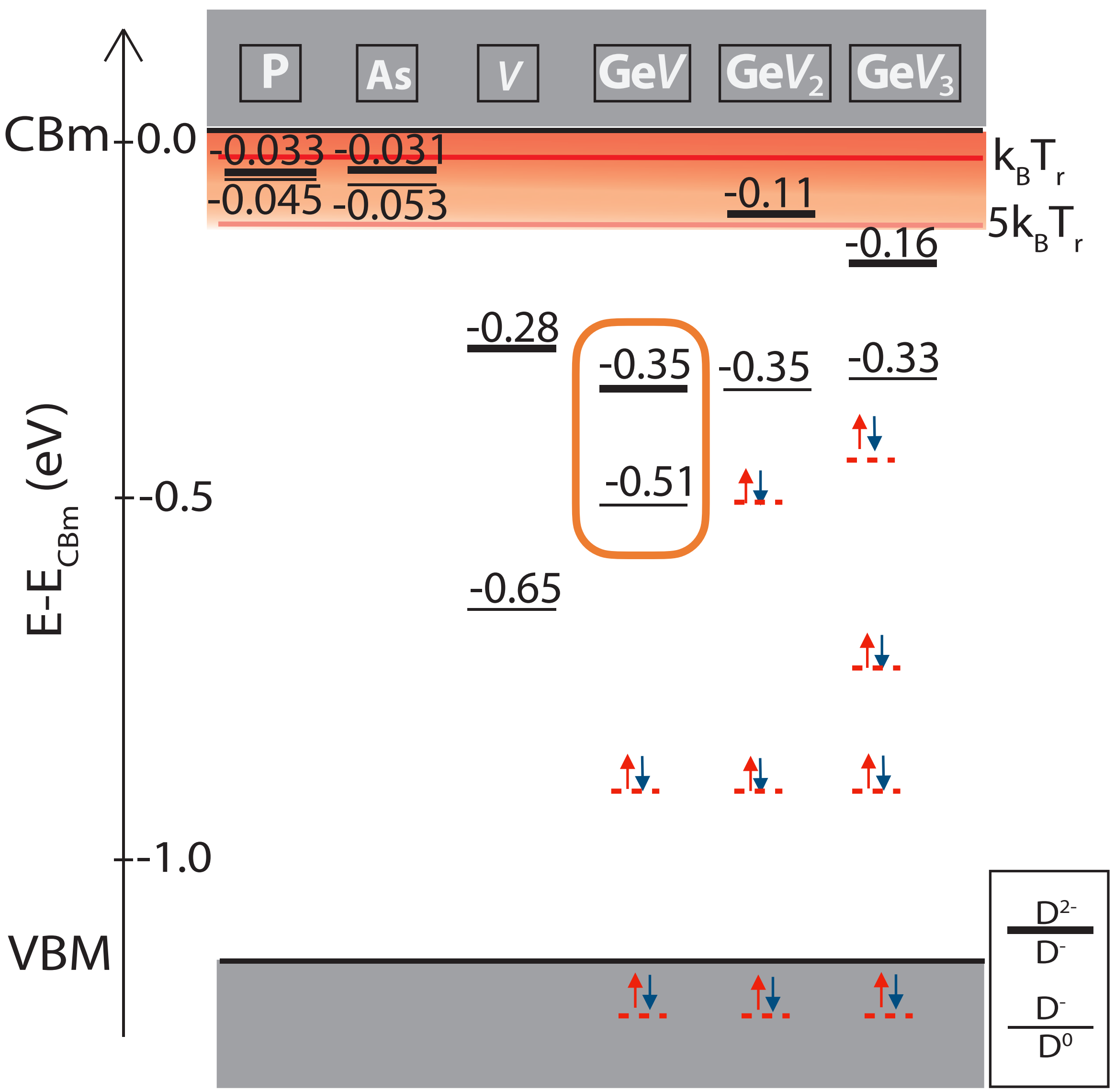

	E_B	E_F
GeV	-0.24	3.95
GeV_2	-2.5	5.95
GeV_3	-4.74	7.93

Deep Level Transient Spectroscopy experiments

Defect	Energy position in gap [eV]	Temperature region [°C]	Proposed identification
E(0.17)	$E_c - 0.17$	up to 600	(O–V)
E(0.21)	$E_c - 0.21$	up to 600	(V–V)
E(0.41)	$E_c - 0.41$	up to 600	(P–V) + (V–V)
E(0.28)	$E_c - 0.28$	400–900	Ge-related
E(0.53)	$E_c - 0.53$	400–900	Ge-related

Y. Suprun-Belevich et al. 1997

S. Achilli, N. Manini, G. Onida, T. Shinada, T. Tanii, E. Prati: Sci. Rep. 8, 18054 (2018)

Electronic properties - Charged excitations

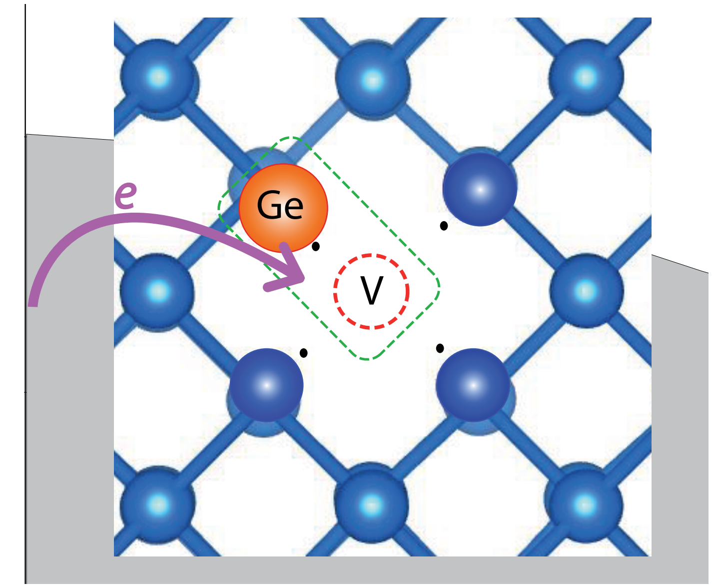

Charge transition levels $\varepsilon(q|q') = \dfrac{E_F(q)-E_F(q')}{(q-q')} - E_{VBM}$

Janak theorem $E_F(q) - E_F(q') = \int_0^1 e_{LUMO}(N+n)dn$

$$E_F(q)-E_F(q') = \frac{e_{LUMO}(N)+e_{HOMO}(N+1)}{2}$$

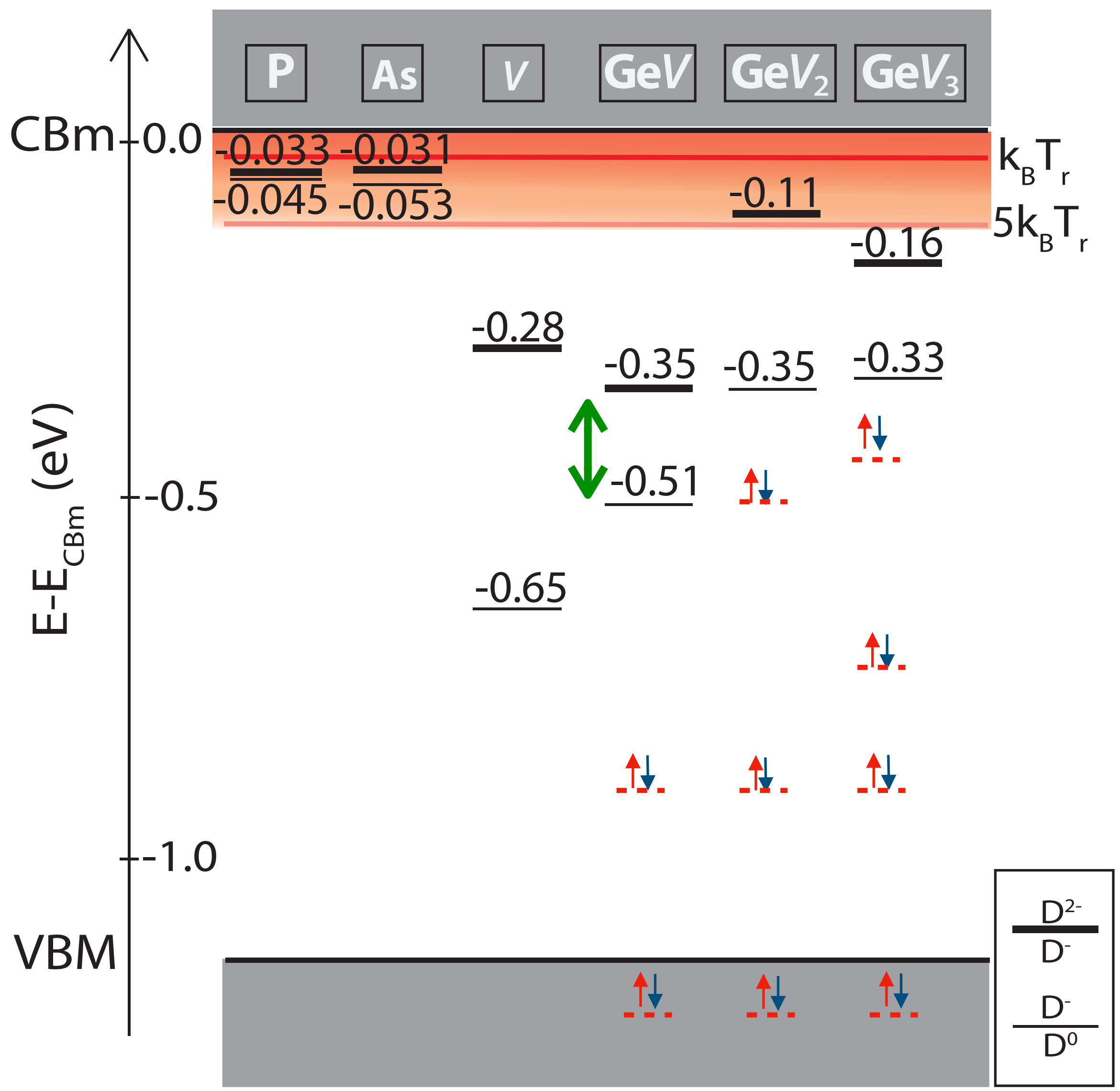

Large electron correlation (**U~150 meV**)

Localized wave function

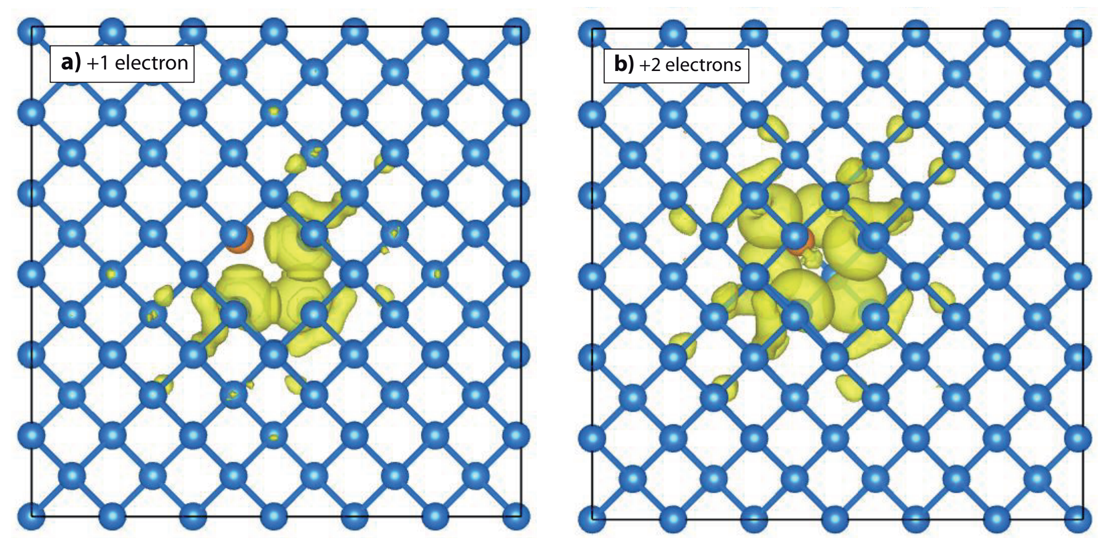

Decay length a_0~ 0.45 nm (1.8 nm for P)

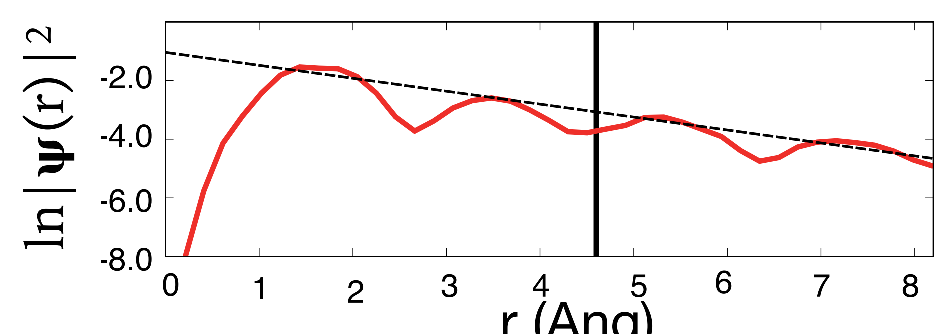

Hubbard model

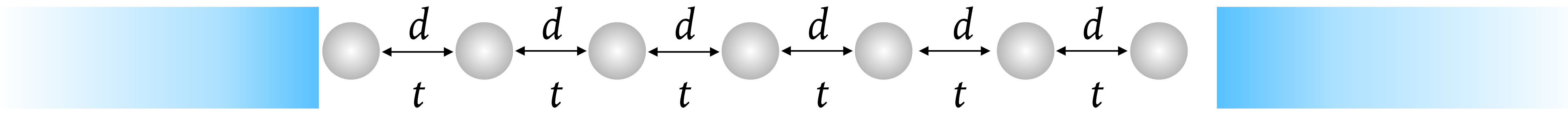

$$H_{\text{array}} = \sum_i \epsilon_i n_i - \sum_{\langle ij \rangle} \sum_{\sigma=\uparrow,\downarrow} t_{ij}(c^\dagger_{i\sigma} c_{j\sigma} + c^\dagger_{j\sigma} c_{i\sigma}) + U \sum_i n_{i\uparrow} n_{i\downarrow} + \sum_{i \neq j} W_{ij} n_i n_j,$$

Ab-initio derived parameters

U=150 meV

$\epsilon_i = -E_B = -0.5eV$

t, W:2-centers integrals
(ab initio wave function)

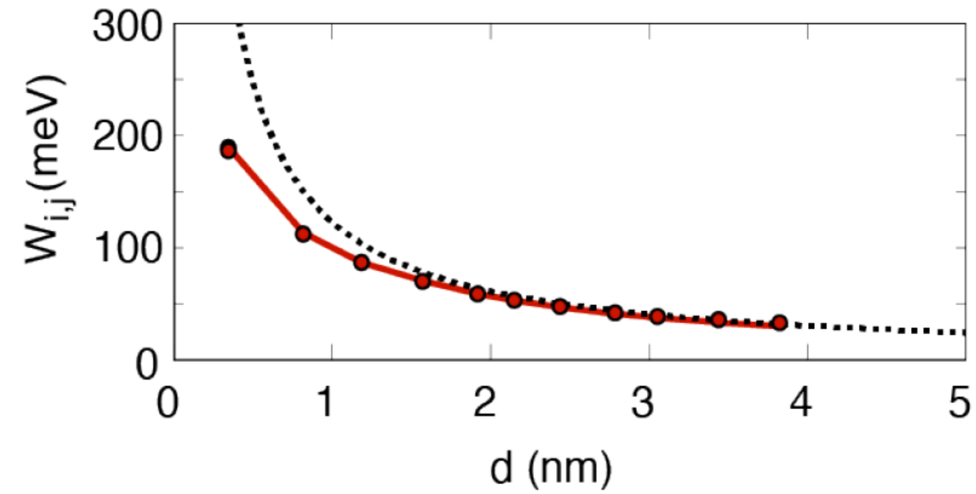

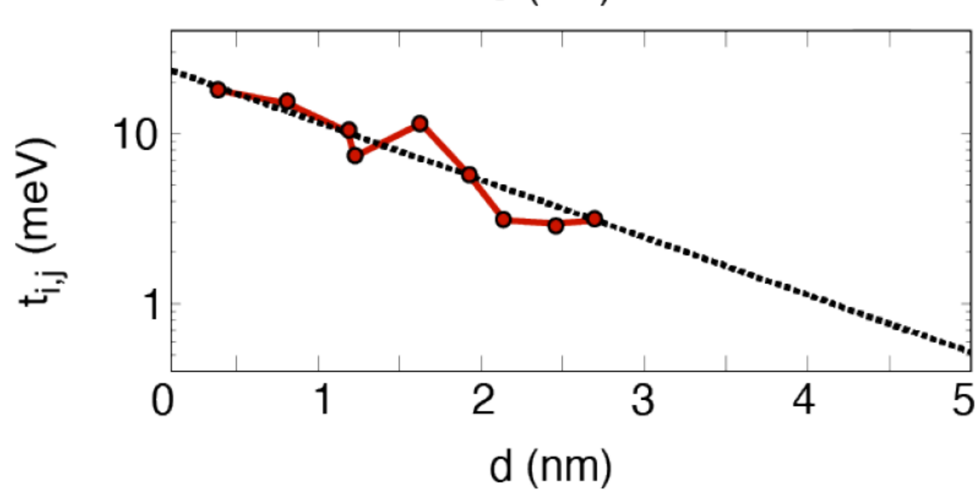

ab initio $|\Psi(r)|$ *for Si:GeV*

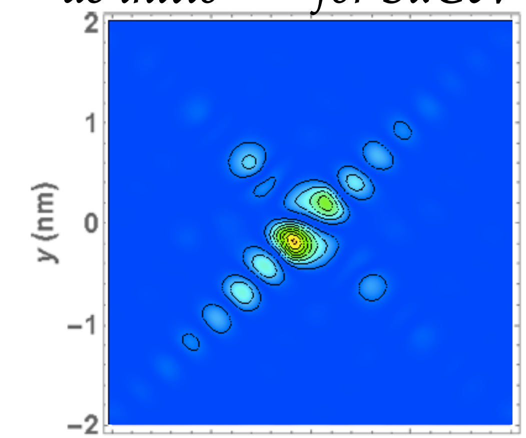

Kohn-Luttinger for Si:P

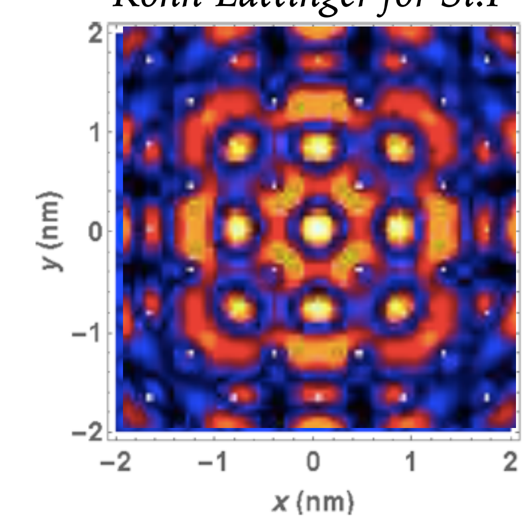

Electronic transport

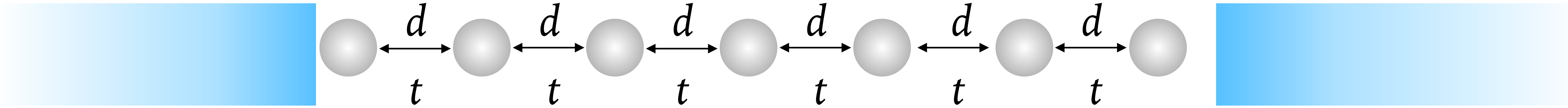

$$H_{\text{array}} = \sum_i \epsilon_i n_i - \sum_{\langle ij \rangle} \sum_{\sigma=\uparrow,\downarrow} t_{ij}(c_{i\sigma}^\dagger c_{j\sigma} + c_{j\sigma}^\dagger c_{i\sigma}) + U \sum_i n_{i\uparrow} n_{i\downarrow} + \sum_{i \neq j} W_{ij} n_i n_j,$$

$$H_{\text{leads}} = \sum_{k\sigma} \epsilon_{k\sigma}^{(R)} c_{k\sigma}^\dagger c_{k\sigma} + \sum_{k\sigma} \epsilon_{k\sigma}^{(L)} c_{k\sigma}^\dagger c_{k\sigma}$$

$$H_{\text{coupling}} = \mathcal{V} \left[\sum_{k\sigma, j \in \text{cL}} (c_{k\sigma}^\dagger c_{j\sigma} + \text{H.c.}) \times \sum_{k\sigma, j \in \text{cR}} (c_{k\sigma}^\dagger c_{j\sigma} + \text{H.c.}) \right]$$

Transition-rate equation

$$G = g_T \sum_{n_\sigma, n_{\bar{\sigma}}} \sum_{\alpha,\beta,\sigma} \frac{M_{\alpha,\beta,\sigma}^{(L),n_\sigma,n_{\bar{\sigma}}} M_{\alpha,\beta,\sigma}^{(R),n_\sigma,n_{\bar{\sigma}}}}{M_{\alpha,\beta,\sigma}^{(L),n_\sigma,n_{\bar{\sigma}}} + M_{\alpha,\beta,\sigma}^{(R),n_\sigma,n_{\bar{\sigma}}}} \times P_\alpha^{n_\sigma,n_{\bar{\sigma}}} \left[1 - f_{FD}\left(E_\alpha^{n_\sigma,n_{\bar{\sigma}}} - E_\beta^{n_\sigma-1,n_{\bar{\sigma}}} - \mu\right)\right]$$

Tunneling rate from left to right

$$M_{\alpha,\beta,\sigma}^{(L),n_\sigma,n_{\bar{\sigma}}} = \sum_{j \in cL} \left| \left\langle \Psi_\alpha^{n_\sigma,n_{\bar{\sigma}}} \middle| c_{j\sigma}^\dagger \middle| \Psi_\beta^{n_\sigma-1,n_{\bar{\sigma}}} \right\rangle \right|^2$$

Positional disorder included (variable hopping)

Energy dependent coupling to the electrodes

N. H. Le et al. Phys. Rev. B 96, 245406 (2017)

Role of disorder - coupling to the electrodes

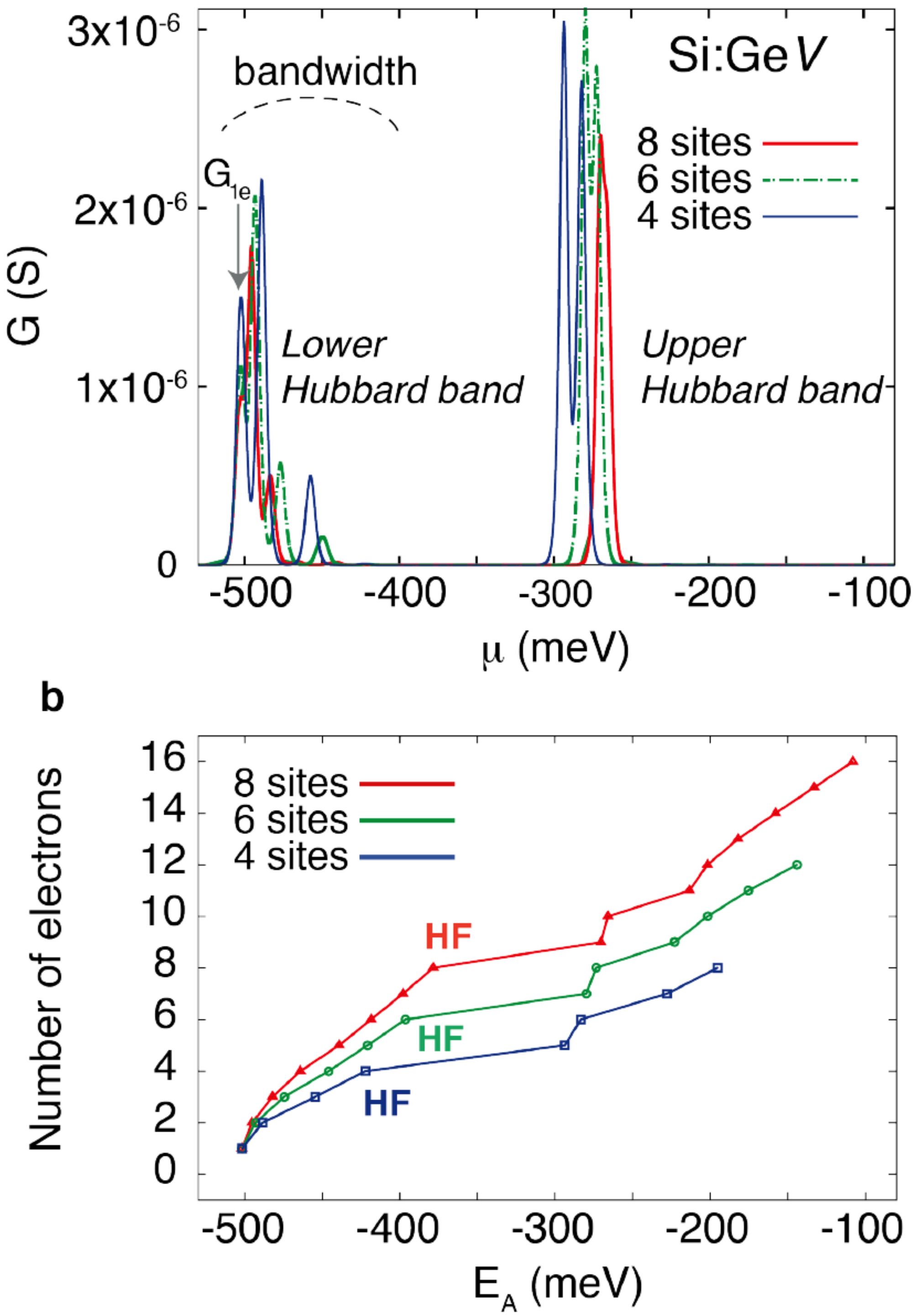

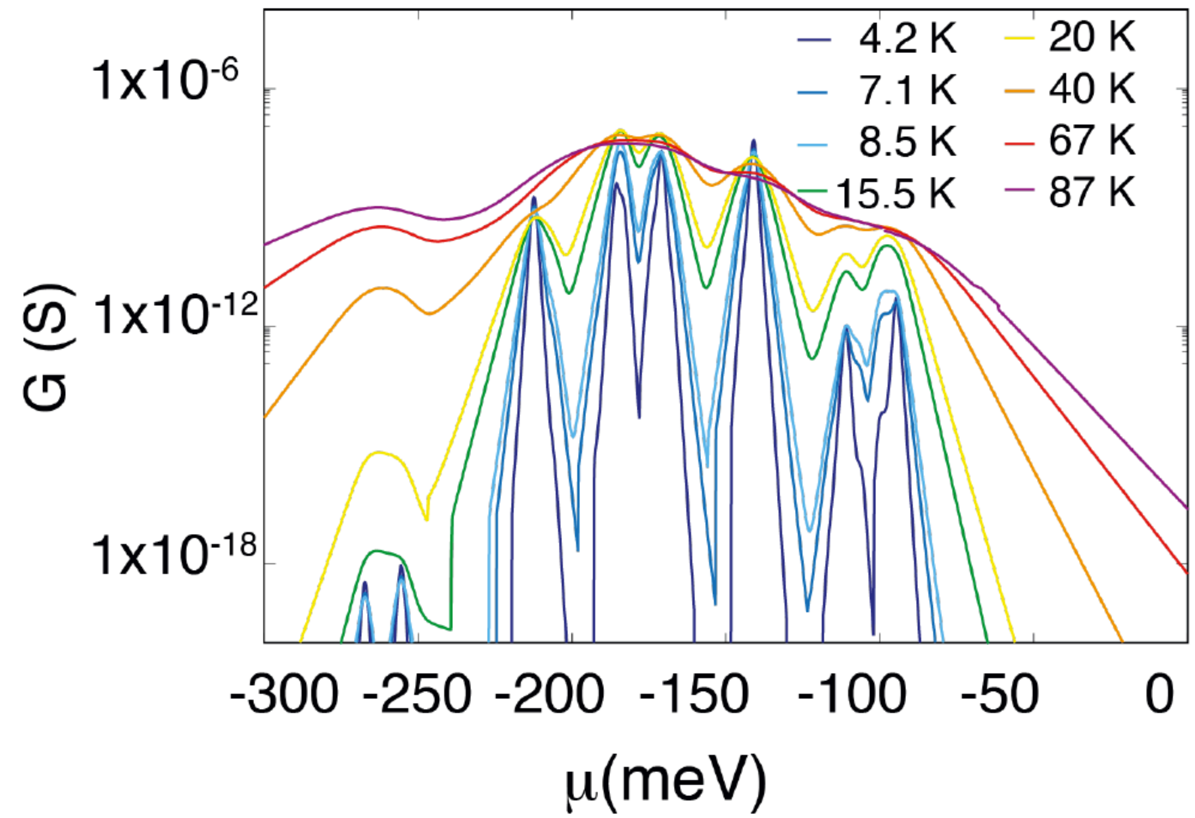

Peaked features in the conductance —> addition of an electron in the chain

Disorder + energy dependent coupling to the leads —> drop of conductivity

S. Achilli *et al.* Adv. Funct. Mater. 31, 2011175 (2021)

Comparison with experimental trans-characteristic

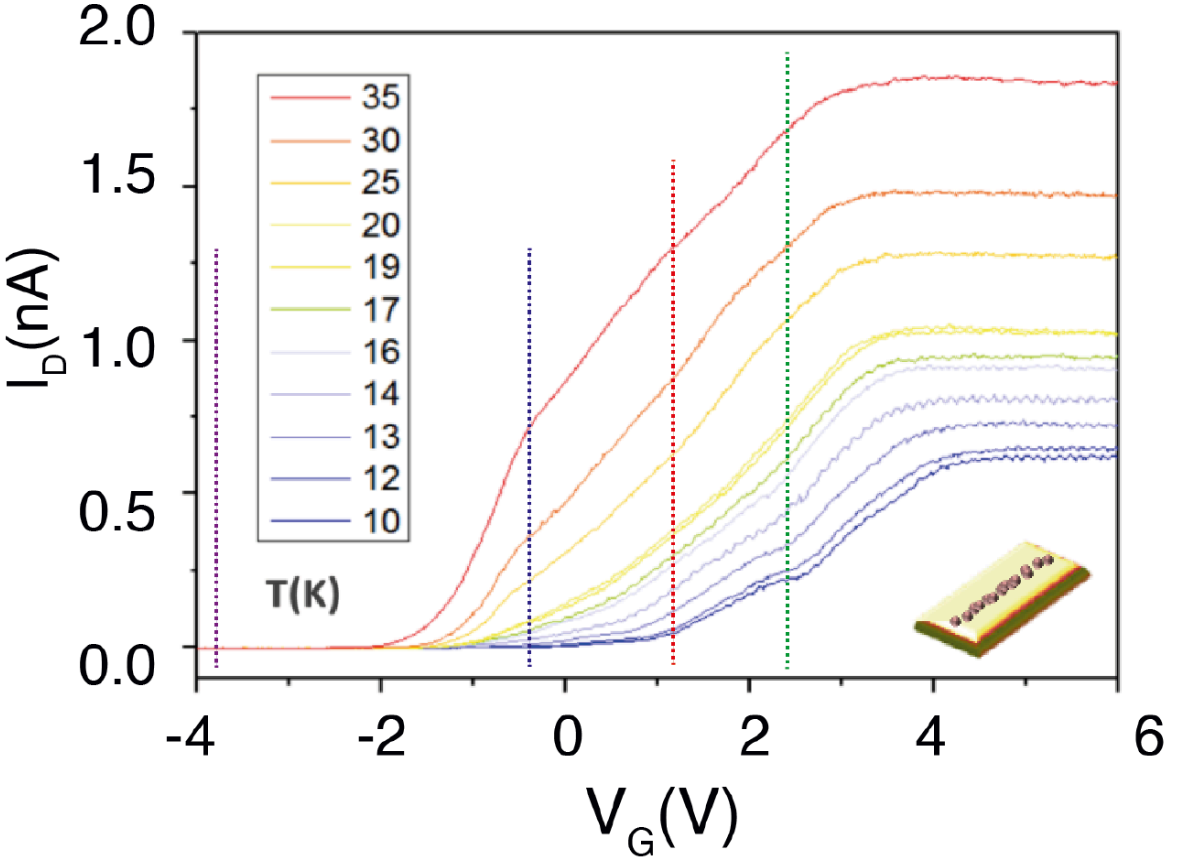

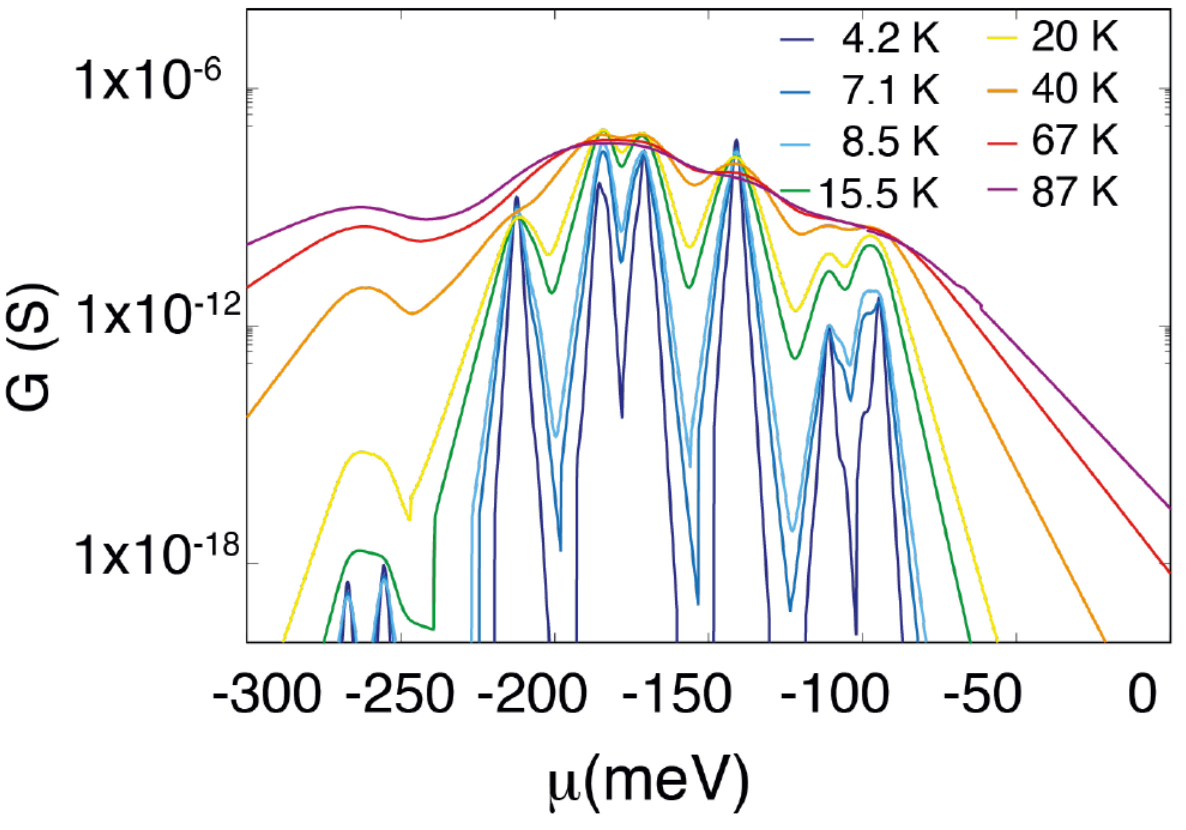

Only the upper Hubbard band is visible in the experiments

Theory reproduces the temperature activated conductivity

Activation energies extracted from the Arrhenius law $\ln G(T) = -E_a/(k_B T) + \text{const}$

S. Achilli *et al.* Adv. Funct. Mater. 31, 2011175 (2021)

EXPERIMENTS

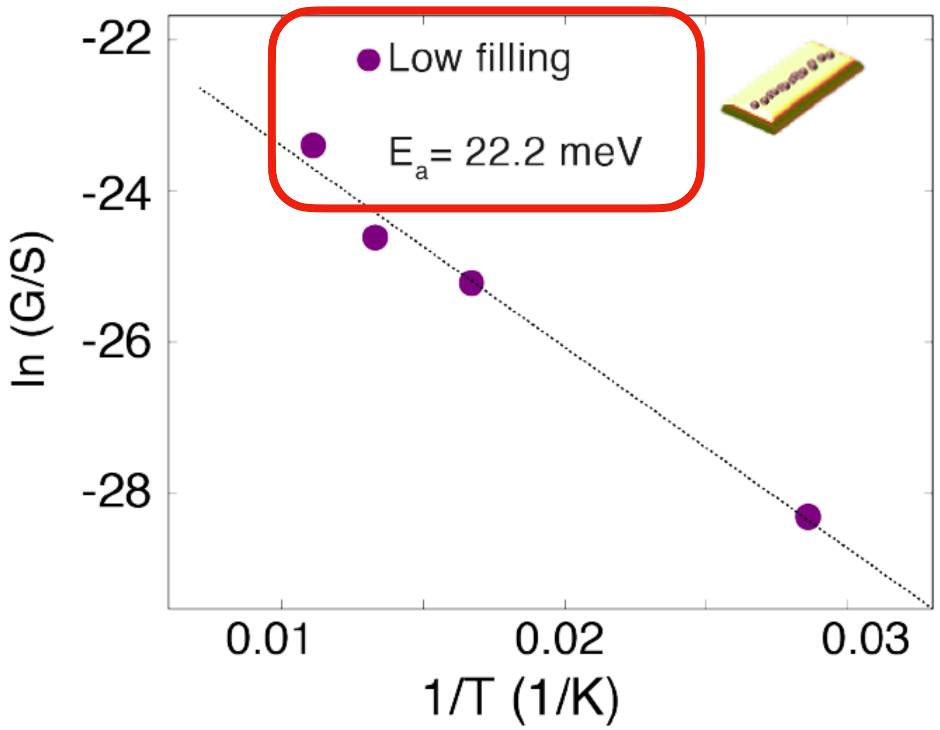

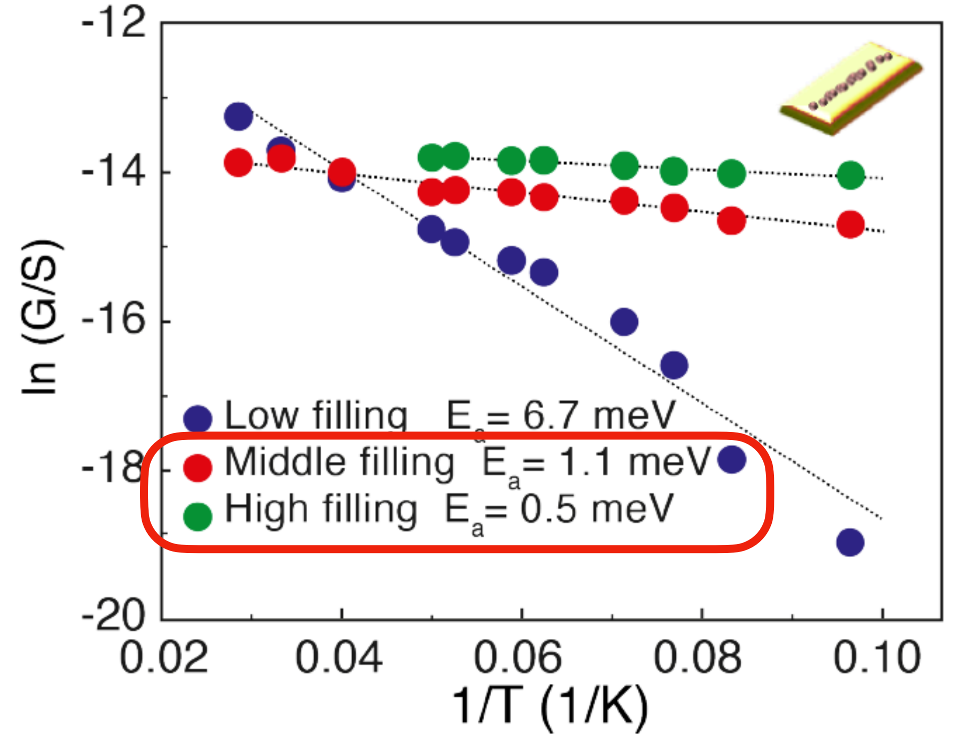

$$\ln G(T) = -E_a/(k_B T) + \text{const}$$

Very high E_a at low filling/high temperature
Very small E_a at high filling/low temperature

Same behavior in the long-channel sample

THEORY

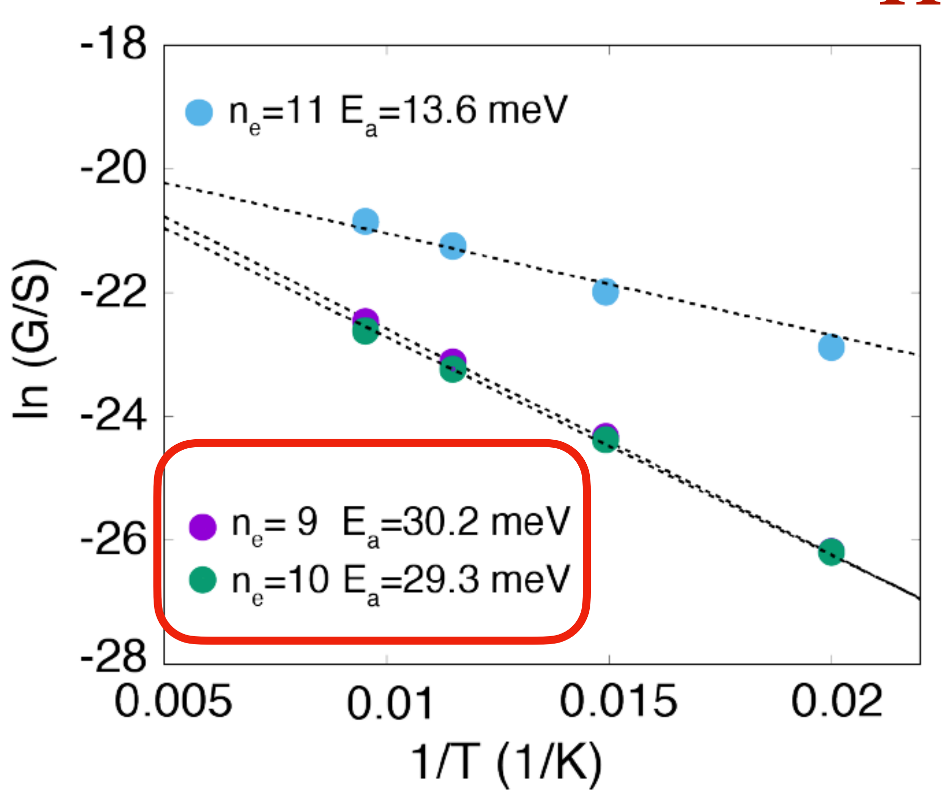

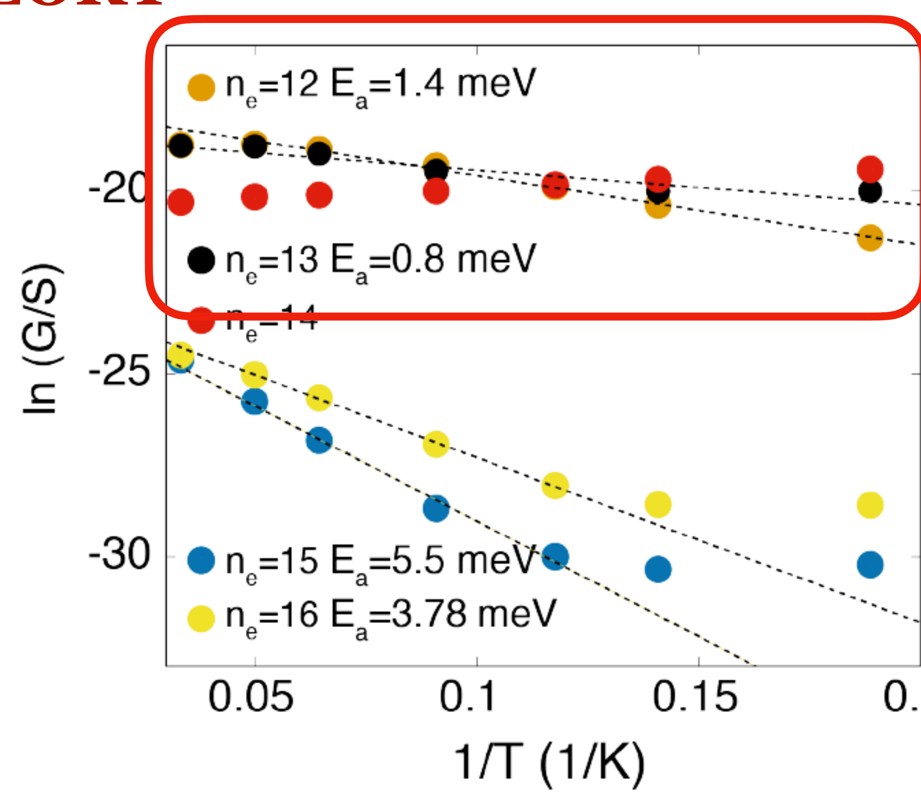

S. Achilli et al.
Adv. Funct. Mater. 31, 2011175 (2021)

The model reproduces the experimental findings —> confirmed by a statistical analysis on different disorder configurations

GeV versus P

- Large U/t ratio in GeV —> more sensitive to localization effects
- GeV is a neutral defect in the ground state:
  Single electron transport enabled in the empty chain, disfavored in the upper Hubbard band

*Single electron-**lower** Hubbard band*

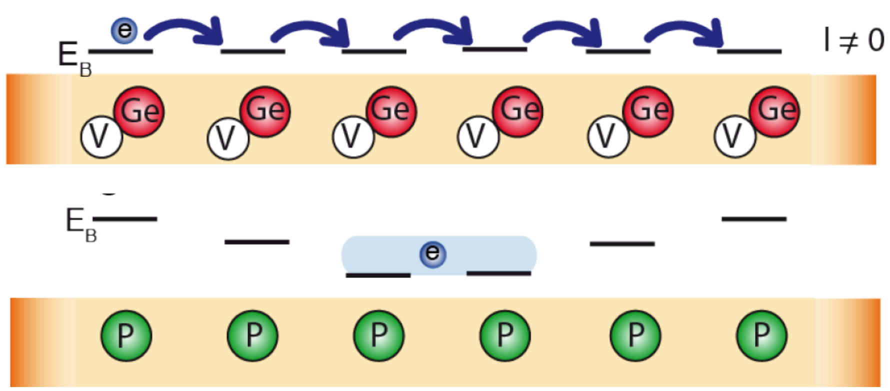

*Low filling - **upper** Hubbard band*

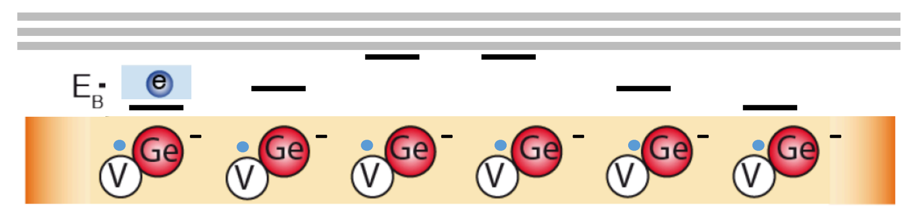

*High filling - **upper** Hubbard band*

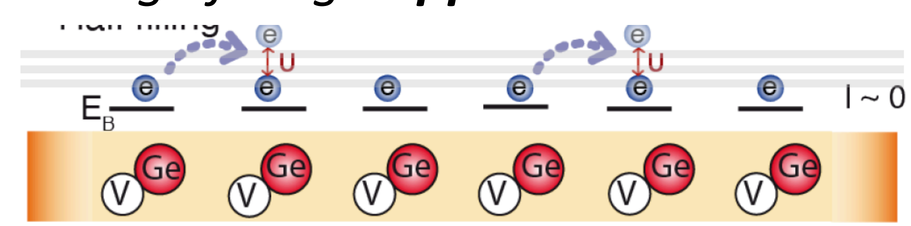

- Negligible temperature dependence at high filling —> transport aided by on-site repulsion (spread of WF)

Conclusion

- Experimental protocol for Ge implantation and generation of GeV complexes
- Multiscale theoretical approach able to catch the main physical properties of GeV
- Agreement with the experiments: both evidence different quantum transport regimes
- Quantum transport results from the balance of Coulomb repulsion and localization
- Temperature activated behavior

Application and perspectives

- Array of GeV defects in silicon: Hubbard simulator
- Single defects —> qubits —> manipulation of quantum information

Aknowledgements

Giovanni Onida
University of Milan

Takashi Tanii
Waseda University

Enrico Prati
IFN- CNR

Nicola Manini
University of Milan

Takahiro Shinada
Tohoku University

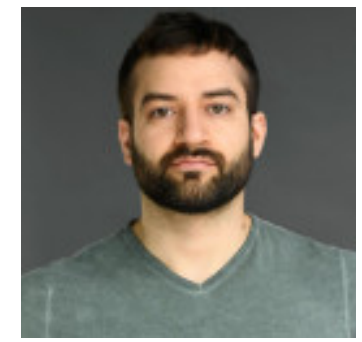

Marco Turchetti
MIT

Guido Fratesi
University of Milan

Nguyen H. Le
University of Surrey

Giorgio Ferrari
POLIMI

Softwares

CRYSTAL — a computational tool for solid state chemistry and physics

siesta™

Grants

nffa.eu — nanoscience foundries & fine analysis

CINECA

Thank you for your attention!